Gough et al. Micro and Nano Systems Letters (2015) 3:4
DOI 10.1186/s40486-015-0017-z

Micro and Nano Systems Letters
a SpringerOpen Journal

LETTER Open Access

# Rapid electrocapillary deformation of liquid metal with reversible shape retention

Ryan C Gough*, Andy M Morishita, Jonathan H Dang, Matthew R Moorefield, Wayne A Shiroma and Aaron T Ohta

**Abstract**

A low-voltage, low-power method of electrically deforming a liquid-metal droplet via the direct manipulation of its surface tension is presented. By imposing a quasi-planar geometry on the liquid metal, its sensitivity to electrocapillary actuation is increased by more than a factor of 40. This heightened responsiveness allows the liquid metal to be deformed at rates exceeding 120 mm/s, greater than an order of magnitude faster than existing techniques for electrical deformation. Significantly, it is demonstrated how this process can be combined with voltage-controlled oxide growth on the surface of non-toxic, gallium-based liquid metals to reversibly form and maintain arbitrary, high-energy shapes.

**Keywords:** Liquid metal; Electrocapillarity; Reconfigurable devices

## Introduction

Liquid metals are an attractive material choice for designers wishing to combine the advantages of metals, such as high electrical conductivity, thermal conductivity, and reflectivity, with the inherently dynamic nature of fluids. Liquid metals have been utilized for a wide variety of applications, including reconfigurable antennas [1] and filters [2], optical switches [3], and wearable electronics [4], among others.

While many of these devices require hydraulic pressure to actuate the liquid metal, there are size, power, and cost advantages in replacing pumps with electrokinetic actuation. Electrowetting on dielectric (EWOD) can create modest deformations in liquid metal by applying electrostatic fringing fields around the edges of the droplet, but at the cost of high actuation voltages [5]. Surface-tension-based actuation techniques such as continuous electrowetting (CEW) are effective at transporting finite volumes of liquid metal with low-voltage, low-power signals [6], although they have not been shown to effectively manipulate the shape of the liquid metal. Liquid gallium and gallium-based alloys have demonstrated large-scale deformation when subjected to small oxidative voltages [7] in what has recently been demonstrated to be an electrochemical reaction [8], but this process generates gallium oxide that can leave residue on channel walls.

Here, we introduce a novel method of electrical surface-tension manipulation that can quickly and dramatically deform a liquid-metal droplet via electrocapillary actuation (ECA). The liquid metal (Galinstan, a non-toxic gallium alloy [9]) is immersed in an electrolyte and enclosed in a reservoir whose width is much greater than its height. This maximizes the surface area of the liquid-metal droplet relative to its volume, making it more responsive to surface-tension-based actuation. Variations in the liquid-metal surface tension are created by applying a small DC bias (referenced to the liquid metal) across the interface between the liquid metal and a surrounding electrolyte. Direct electrical surface-tension manipulation has been previously used to actuate liquid metal, but with modest deformation [10]. Here, it is shown that the sensitivity of the liquid metal to electrical manipulation can be greatly heightened by imposing a quasi-planar geometry, which substantially decreases the excess surface energy required for actuation and increases responsiveness by over an order of magnitude. The authors have previously used this technique to tune the passband of a coupled-line bandpass filter by elongating the liquid-metal central resonator [11].

Electrocapillary actuation requires low voltage and low power, is immediately reversible, results in a greater deformation than EWOD, and is capable of moving liquid

* Correspondence: rgough@hawaii.edu
Department of Electrical Engineering, University of Hawaii at Manoa, Honolulu, Hawaii 96822, USA

metal at speeds of over 120 mm/s. Furthermore, when gallium-based alloys such as Galinstan are used, the application of oxidative potentials results in oxide growth [8] that can be used as a reversible means of maintaining the liquid-metal surface deformation created by ECA. It was previously shown that the natural oxidation of gallium alloys can be leveraged as mechanical support in the creation of 3D structures [12]. Here, we propose using voltage-controlled oxidation to create mechanical support for induced deformations that can be turned on and off like a switch. The technique described in this paper follows this process: first, Galinstan is rapidly deformed with ECA. Second, the deformed Galinstan is held in place by the sudden application of an oxidative potential. Finally, the liquid metal remains in this deformed state until the oxidative potential is replaced by a reductive voltage that removes the oxide layer, allowing the Galinstan to return to its minimum-energy geometry (an application of "recapillarity" [13]).

## Findings

### Theory

Liquid metal immersed in an electrolyte develops a net surface charge as a result of ion transfer across the interfacial boundary. This charge attracts opposite ions from the surrounding electrolyte, resulting in the formation of an electrical double layer (EDL) [14]. The surface tension $\gamma$ of the liquid metal is a function of the EDL, as described by the Young-Lippman equation:

$$\gamma = \gamma_o - \frac{1}{2} C V_{EDL}^2, \tag{1}$$

where $\gamma_o$ is the surface tension minus electrical influence, $C$ is the capacitance per unit area of the EDL, and $V_{EDL}$ is the voltage across the EDL [14]. This phenomenon, where surface tension is influenced by electrical conditions at the liquid-liquid boundary, is known as electrocapillarity [15].

The electrical control of surface tension can also adjust the pressure at the interfacial boundary. A pressure differential $\Delta p$ naturally exists between the liquid metal and electrolyte, and is related to the surface tension $\gamma$ by the Young-Laplace equation:

$$\Delta p = \gamma\left(\frac{1}{R_1} + \frac{1}{R_2}\right), \tag{2}$$

where $R_1$ and $R_2$ are the principal curvature radii [16]. Liquid metal in an electrolyte-filled channel has a near-180° contact angle with the channel walls [14], so the pressure is higher within the liquid metal relative to the electrolyte. CEW actuation takes advantage of this relationship by creating a surface-tension gradient across the length of a liquid-metal slug, resulting in a pressure imbalance from one end of the slug to the other and inducing motion [14], [17].

In ECA, the EDL voltage is altered by directly applying a DC bias between the liquid metal and electrolyte. This has the same low-voltage and low-power advantages as CEW, but allows for the liquid metal to be deformed and shaped instead of simply moved from point to point. Previous attempts at utilizing this technique resulted in only minor deformation [10] due to the low surface-area-to-volume ratio of the liquid metal. Here we show how these deformations can be greatly increased by maximizing this ratio.

In the absence of external forces, the surface tension of a liquid droplet works to minimize the surface area, and thus the free surface energy, of the liquid by forming a sphere [16]. Any further increase in this surface area $dS$ requires external work equaling $\alpha dS$, where $\alpha$ is the surface tension of the liquid [16]. If the deformation of a spherical liquid-metal droplet under electrical manipulation is approximated as a transformation of the sphere into a prolate spheroid, the new liquid-metal surface area $S$ can be calculated by

$$S_{spheroid} = 2\pi b^2\left(1 + \frac{a}{be}\sin^{-1}e\right), \tag{3}$$

where $a$ and $b$ are the semi-major and semi-minor axes respectively, and $e$ is the eccentricity of the spheroid, defined as (ref. [18])

$$e = \sqrt{1 - \left(\frac{b}{a}\right)^2}. \tag{4}$$

The axes $a$ and $b$ are further related by the finite volume $V$ of the liquid metal,

$$b = \sqrt{\frac{3V}{4\pi a}}. \tag{5}$$

Using this prolate spheroid approximation, the deformation of the liquid metal can be characterized as a change to the length of the semi-major axis $a$, and the resulting increase in the surface area of the spheroid can be calculated.

Now, consider the same volume $V$ of liquid metal, trapped between two plates separated by height $h$, where $h$ is much smaller than the original spherical radius $r$. The surface tension minimizes the free surface energy of the liquid metal as before, but with the new quasi-planar boundary conditions imposed by the plates, the optimum shape is now a flattened cylinder with height $h$ and facial radii $R$ (the curvature of the walls of the cylinder is assumed to be negligible compared to $R$). The surface area of this cylinder can be expressed generally as

$$S_{cylinder} = 2\pi R^2 + Ph, \tag{6}$$

where the general term $P$ is used for the perimeter. In the minimum-energy case $P$ is the circumference of the cylinder, $2\pi R$.

The majority of the surface area of the cylinder is comprised of the circular faces at each of the two planar boundaries. Furthermore, if $h$ is held constant and the deformation of the liquid metal is limited such that the equivalent semi-minor spheroid axis $b$ is always much greater than $h$, then the area of these faces remains constant. That is, deformation of the liquid metal transforms these circles into ellipses and increases the perimeter length $P$, but does not alter the area of the liquid metal in contact with each plate.

This is significant because the product $P \times h$ is a small percentage of the overall surface area of the cylinder, so even dramatic liquid-metal deformations require only a very small increase in surface energy. This effect is illustrated in Figure 1, which plots the extent that the semi-major axis of the liquid metal can be elongated as a function of the required change in normalized surface energy. The smaller the height $h$ between the planar boundaries becomes, the smaller the excess surface energy that is required for deformation. This in turn makes the liquid metal much more responsive to perturbation: for example, given a constant change in surface energy, a volume of liquid metal flattened such that its cylindrical height $h$ becomes 10% of the original spherical radius will elongate approximately 40 times further than it would if the same surface energy change was applied to the original sphere.

Figure 2 shows a top-view illustration of a liquid-metal droplet trapped in a quasi-planar ($R >> h$) reservoir filled with an alkaline electrolyte. The reservoir is connected to a long, narrow channel of the same height, which is also filled with the electrolyte. A smaller pressure-relief channel extends from the reservoir in the opposite direction, which allows the liquid metal to flow into the larger channel without creating negative pressure at its trailing edge. In ambient conditions the liquid metal is trapped in the reservoir, as opposing capillary forces block flow into either channel.

At the end of the primary channel opposite the reservoir, a positive voltage is applied to the electrolyte relative to the liquid metal. As the electrolyte is semi-conductive, a potential gradient is established within the channel and along the interface between the electrolyte and liquid metal. This creates a surface-tension gradient along the interfacial boundary as described by (1), with the lowest surface tension at the channel entrance. Marangoni forces ($F_{Mar}$) that develop along this interface generate a flow of the electrolyte away from the channel entrance, and exert negative displacement pressure on the liquid metal, pulling it flush across the channel entrance. Entrance of the liquid metal into the channel is opposed by the capillary pressure of the channel; this additional pressure threshold must be overcome if flow is to be initiated.

From (2), the pressure discontinuity $p$ of the liquid metal relative to the surrounding electrolyte within the reservoir can be described as:

$$p_{reservoir} = \gamma_{t=0}\left(\frac{1}{R} + \frac{2}{h}\right), \tag{7}$$

where $\gamma$ is the initial surface tension prior to electrical actuation, and $R$ and $h$ are the radius and height of the reservoir, respectively. The vertical curvature radius can be approximated as half the reservoir height because the

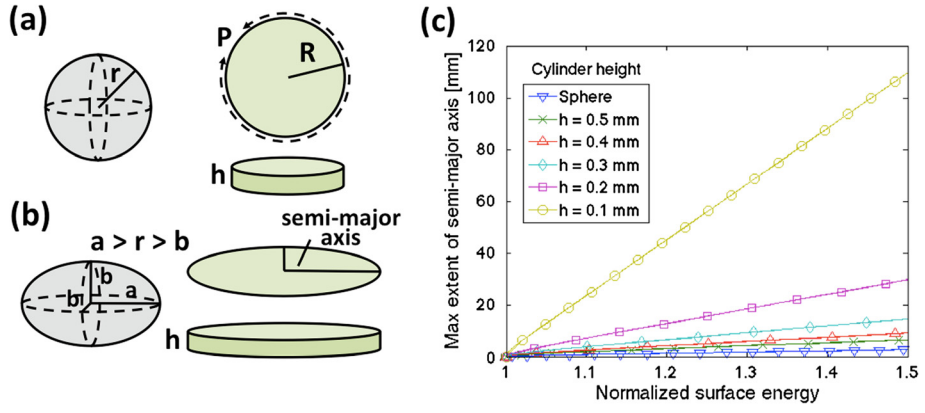


**Figure 1 Effects of confinement on surface energy increase required for deformation. (a)** A finite volume of liquid metal (or any liquid) minimizes its surface energy by contracting into a sphere with radius $r$. Flattening this sphere leads to a cylinder with facial radius $R$ and perimeter $P$. **(b)** Elongating the liquid sphere can be approximated as transforming it into a prolate spheroid whose semi-major axis $a$ is longer than both the original radius $r$ and the semi-minor axis $b$. This action necessarily involves increasing its surface area, and thus its free surface energy. Similarly distorting the cylinder will transform it into an ellipse, but its semi-major axis will lengthen by a much larger amount for the same change in overall surface energy. **(c)** Calculated maximum deformation of a liquid-metal spherical droplet with a 1-mm radius as it is compressed into a cylinder of varying heights. As the liquid metal is flattened it is capable of much greater deformation for a given increase in its surface energy.

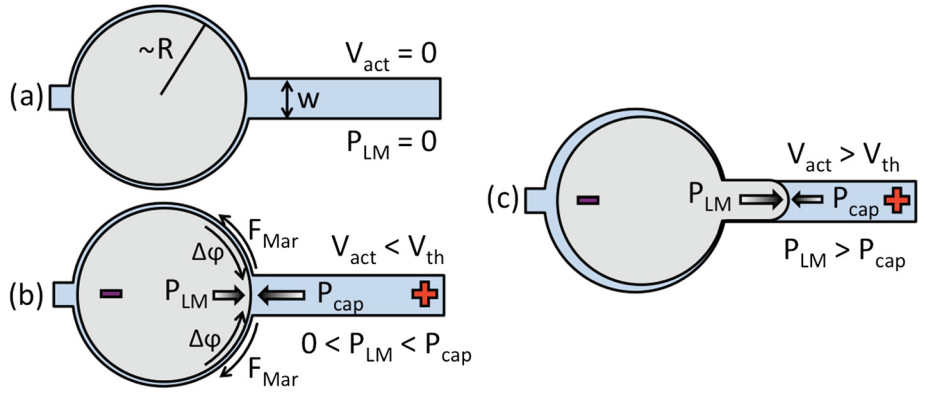


**Figure 2 Electrocapillary actuation of liquid metal. (a)** Liquid metal resting in a quasi-planar reservoir exerts no lateral pressure. **(b)** A positive DC voltage creates a potential gradient on the liquid-metal surface near the primary channel entrance, resulting in a corresponding surface-tension gradient and generating Marangoni forces. The liquid metal now exerts a positive pressure on the channel entrance that is opposed by the channel's capillary pressure. **(c)** Above the critical voltage threshold, the pressure exerted by the liquid metal exceeds the capillary pressure, and the liquid metal enters the channel. Flow is facilitated by the pressure-relief channel at the opposite end of the reservoir, which prevents a negative pressure build-up at the trailing edge of the liquid metal.

contact angle at the liquid-liquid–solid interface is approximately 180°.

To induce flow into the channel, the pressure exerted by the liquid metal must exceed the capillary resistance of the channel. The pressure differential of the liquid metal within the channel once this occurs is:

$$p_{channel} = 2\gamma_1\left(\frac{1}{w}+\frac{1}{h}\right), \tag{8}$$

where $\gamma_1$ is the reduced surface tension resulting from the applied bias potential and $w$ and $h$ are the width and height of the channel, respectively. At the threshold point, these pressures are equal, and so by combining (7) and (8) we can determine the normalized surface tension at which flow is induced:

$$\hat{\gamma} = \frac{\gamma_1}{\gamma_{t=0}} = \frac{w(h+2R)}{2R(h+w)}. \tag{9}$$

This equation can be re-written in terms of the channel aspect ratio $h/w$, and approximated for conditions when $h/2R$ is negligibly small:

$$\hat{\gamma} = \frac{1}{{}^{h}/_{w}+1}\cdot\left(1+\frac{h}{2R}\right) \approx \frac{1}{{}^{h}/_{w}+1}. \tag{10}$$

Figure 3 shows this normalized surface tension plotted as a function of channel geometry for a reservoir radius of 5 mm. For channels that have a small aspect ratio ($h/w$), very little reduction in surface tension is required to induce flow: for a channel with a width of 3 mm and a height of 0.1 mm, a normalized surface tension of approximately 97% will result in liquid-metal deformation due to electrocapillary actuation. As the channel aspect ratio is increased, a greater reduction in surface tension is required, which in turn requires higher actuation voltages. The relationship between normalized surface tension and channel aspect ratio, approximated for cases in which $h/2R$ is negligibly small, is plotted as an inset in Figure 3.

### *Experiment*

A series of test fixtures was fabricated consisting of a single cylindrical reservoir with a 5-mm radius connected to one or more channels extending outward from the reservoir (Figure 4). The walls of the test fixture are fabricated from polyimide tape, with a glass floor and ceiling. The channels have a constant height $h$ and width $w$ through which the liquid metal can flow, and are

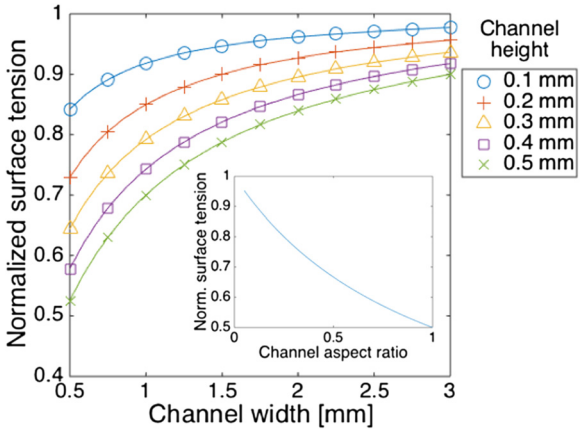


**Figure 3 Normalized surface tension required for flow of liquid metal.** Minimum normalized surface tension required to initiate flow for liquid-metal in a cylindrical reservoir into a channel of a given height and width. The assumed reservoir radius is 5 mm. Inset: approximate normalized surface tension required for flow as a function of channel aspect ratio $h/w$.

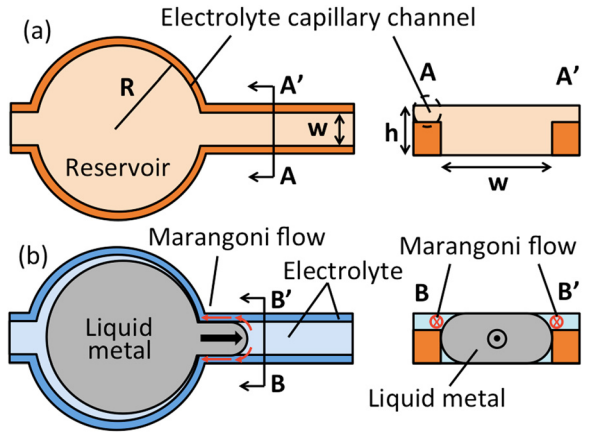


**Figure 4 Primary channel with capillary side-channels to facilitate electrolyte backflow. (a)** Primary channels extending from the reservoir have a constant height *h* and width *w*. Two small capillary channels frame each primary channel. **(b)** When the electrolyte is introduced it fills both the primary and capillary channels, whereas the liquid metal remains only in the primary channel. During ECA actuation Marangoni forces cause the electrolyte to flow in the opposite direction of the liquid metal, and the capillary channels provide the electrolyte with an unobstructed path into the reservoir.

framed by two small capillary channels that allow entry to the electrolyte but not the liquid metal. This is important, as Marangoni forces caused by the surface tension gradient at the liquid-metal/electrolyte interface can result in strong backflow of the electrolyte. Without these capillary channels, the flow of the electrolyte can become obstructed by the bulk liquid metal, hindering the flow speed of the liquid metal.

The reservoir and channels are filled with a solution of 1% NaOH, after which the reservoir is filled with Galinstan. The Galinstan wets to a 1-mm-wide embedded copper strip that extends approximately 3 mm into the reservoir, and connects to an external probe point. The probe, along with a graphite probe at the opposite end of each channel, is used to apply an electrical bias directly across the interface between the electrolyte and liquid metal.

A negative DC bias relative to the Galinstan droplet leads to oxide growth on the surface of the liquid metal [8]. The oxide growth is primarily located on the surface facing the channel opening, where the oxidative potential relative to the electrolyte is greatest. The hydrophilic nature of this oxide leads it to increase its contact area with the electrolyte [8], and the liquid metal begins spreading outwards into the channel at speeds on the order of 2 to 3 mm/s.

As the Galinstan travels down the channel, it continually breaks through the newly formed oxide layer at the leading edge with fresh bulk liquid metal, which then itself becomes oxidized (Figure 5). If the oxidative potential at the leading edge becomes sufficiently high, the oxide growth becomes rapid enough that the bulk liquid metal is unable to break through. Eventually the liquid metal reaches a critical length beyond which its flow is halted by the thick oxide layer; these critical lengths are detailed in Figure 6, along with images of the halted flow at various applied voltages. There is a linear inverse relationship between applied voltage and critical oxidation length.

Removing the DC bias reasserts the ambient conditions in the channel; the electrolyte reduces the oxidation at the leading edge and, without the mechanical

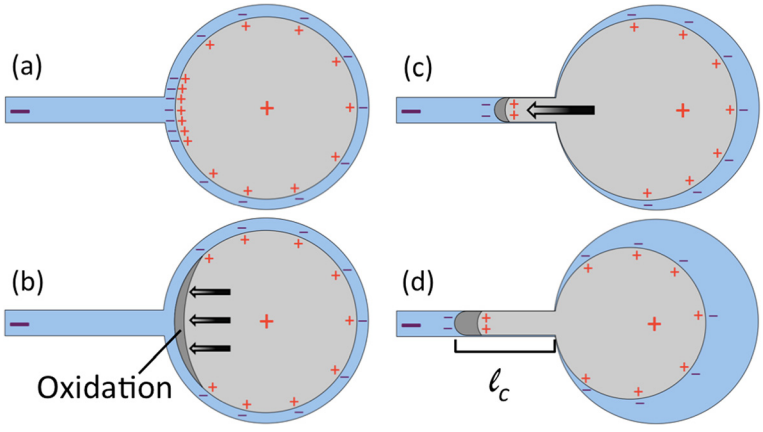


**Figure 5 Electrochemical actuation of liquid metal.** In ambient conditions the liquid metal has a uniform negative surface charge and attracts counter-ions in the alkaline electrolyte. **(a)** This charge distribution is disturbed when an external bias creates a potential gradient in the vicinity of the liquid metal. **(b)** An oxidative reaction is created, especially near the channel opening where the oxidative potential is greatest, and **(c)** the liquid metal begins slowly flowing into the channel. **(d)** At higher potentials the advance is halted at some critical length $l_c$, where the liquid metal cannot break through the rapidly forming oxide layer at the leading edge.

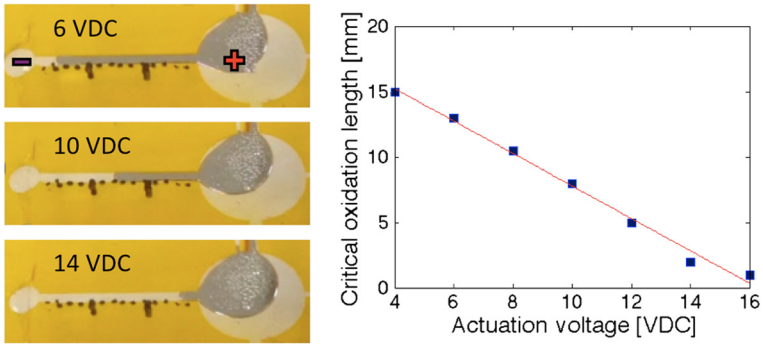


**Figure 6 Critical oxidation lengths.** Critical oxidation lengths for electrochemically actuated liquid metal advancing in a 1 mm x 15 mm x 0.3 mm channel. The images show the maximum length the liquid metal advances into the channel before the oxide formation at its leading edge becomes too rapid to break through. The plot shows the linear relationship between this critical length and the oxidizing actuation voltage.

support provided by the oxide layer, the liquid metal retracts back to its minimum-energy position [13]. The time required for this reduction can vary from tens of seconds to several minutes, depending on how thick the oxide layer has become, which in turn dictates how far into the channel the liquid metal has progressed.

A positive voltage applied to the electrolyte relative to the liquid metal (Figure 2) does not result in an oxidizing reaction, and instead generates a buildup of electrocapillary pressure at the channel entrance. When this pressure exceeds the opposing capillary pressure of the channel, rapid flow of the liquid metal into the channel is initiated. The velocity of this flow is a function of both the channel geometry as well as the induced pressure drop caused by the actuation voltage. Thus, the flow velocity can be controlled either by raising the DC potential or by altering the channel dimensions.

Actuation speeds were measured for liquid metal being drawn into 15-mm long, 0.3-mm deep channels of varying width using both ECA (voltage applied relative to liquid metal) and electrochemical (voltage relative to electrolyte) actuation methods. The measured speeds for ECA (Figure 7)

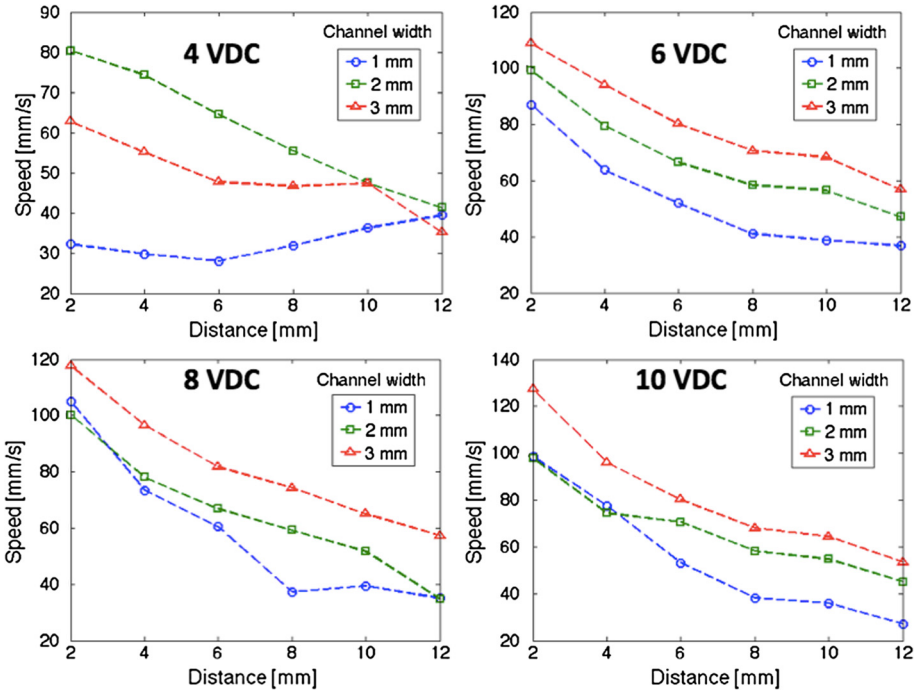


**Figure 7 ECA measured velocities.** Measured ECA actuation speeds for actuation voltages of 4, 6, 8, and 10 VDC. Test channels are 300 μm tall and 15 mm long, with widths that vary as indicated. The reservoir radius for all channels is 5 mm.

vary as a function of the actuation voltage and the channel geometry, but are generally on the order of 100 mm/s as the liquid metal enters the channel. This is much faster than the speed of electrochemical actuation, which our tests measured at approximately 2 to 3 mm/s. Actuation speeds for both processes vary directly with applied voltage, although at 10 VDC and higher rapid bubble generation from electrolysis becomes an issue for both methods. For ECA, narrower channels require a buildup of higher electrocapillary pressure to initiate flow, so increasingly higher actuation voltages are required to achieve the necessary reduction in surface tension. Electrochemical actuation requires no minimum pressure build-up, and begins as soon as the applied potential is sufficient to initiate oxidation.

For all measured channel widths, a minimum applied voltage of 4 VDC was required to initiate reliable liquid metal flow. As the actuation voltages increase, the flow velocities also increase, with a general trend of faster flow rates in wider channels. Wider channels have reduced capillary force opposing the flow of liquid metal into the channel, resulting in faster liquid-metal flow rates as the channel width increases. As the liquid metal travels further into the channel, its progress is opposed by the hydraulic resistance of the channel as well as the contractile force imposed by its own surface tension. These forces slow the liquid metal continuously so that by the time its leading edge has neared the end of the channel, the speed of the liquid metal has generally decreased from 100 mm/s to 40 to 50 mm/s. However, these speeds still mean that the liquid metal is moving at a rate that is greater than an order of magnitude faster than is possible with electrochemical actuation, allowing for electrically controlled deformations that are much more sensitive to electrical stimuli.

ECA and electrochemical actuation are both unique in their ability to dramatically distort and re-form liquid metal using the direct application of low-voltage and low-power signals. Electrochemical actuation is not dependent on channel geometry and thus enjoys a much wider range of possible deformation, but within the quasi-planar geometries described here ECA is a much more rapid process. Furthermore, the relationship between actuation voltage and oxide formation shown in Figure 6 implies that a

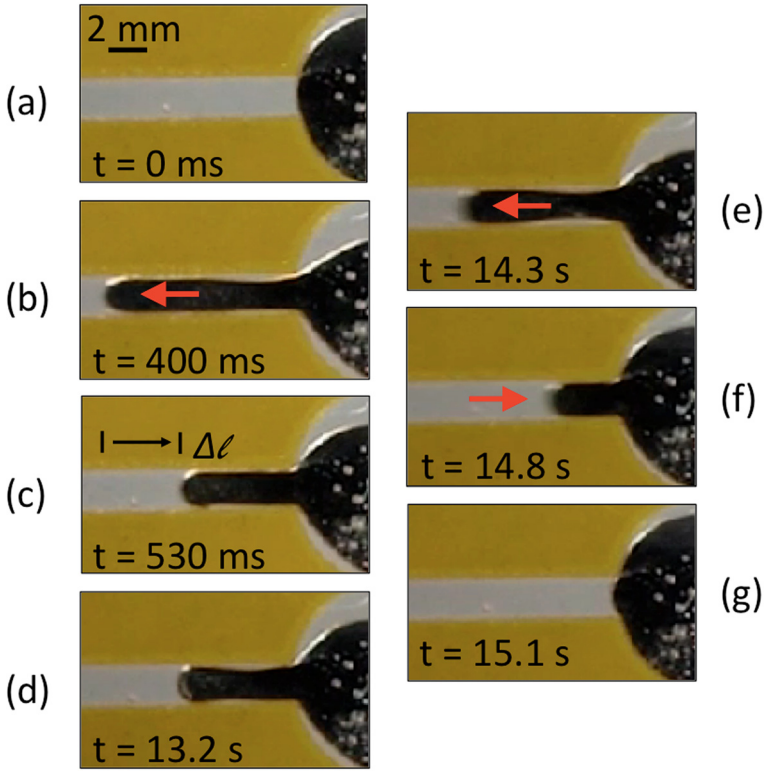


**Figure 8 Sustained, reversible actuation with ECA and voltage-controlled oxidation.** ECA used in conjunction with electrochemical oxide deposition to actuate and control liquid-metal deformations. Liquid metal is actuated by 4 VDC applied to the electrolyte **(a)** and advances quickly into the channel until the bias switches to −10 VDC **(b)**. Liquid metal retracts by ~ 4 mm (Δ*l*) before oxide growth is sufficient to wet to walls and halt movement **(c)**. The liquid metal is allowed to remain in this position for approximately 12 seconds before 4 VDC is again applied to remove the oxide [13] and reverse the deformation **(d)**. The 4-VDC bias restores ECA conditions, causing the liquid metal to advance even before the oxide is fully reduced **(e)**, and so must be applied in short bursts. Eventually the liquid metal recedes as the oxide is removed **(f)**, before finally returning to the central reservoir **(g)**.

sufficiently oxidative voltage can result in oxide growth capable of halting liquid-metal flow in a capillary channel. Since the oxide also wets to the walls of the channel, the liquid metal is trapped in the position in which the strong oxidizing voltage was applied. This is a potentially powerful way of combining ECA with electrochemical oxide deposition; ECA is used to rapidly deform the liquid metal before an oxide layer is developed that provides the mechanical support to maintain the deformation. Reversing the process is achieved by re-applying a small positive bias across the electrolyte relative to the liquid metal ("recapillarity" [13]).

In Figure 8, a 4-VDC signal, referenced to the Galinstan, is applied to the electrolyte to pull the liquid metal into a narrow channel via ECA. Abruptly the signal is reversed to −10 VDC, resulting in rapid oxide formation at the leading edge of the liquid metal. The Galinstan begins contracting back to the reservoir, but this contraction is quickly halted by the newly formed oxide layer, which wets to the channel walls and locks the liquid metal into a position that would otherwise require an unsustainable amount of free surface energy.

The liquid metal will remain in this position as long as the adhesive force between the oxide and the channel walls is sufficient to overcome the contracting force of the liquid metal. The prolonged application of the oxidizing voltage will continuously grow the oxide layer, and while this can increase the mechanical stability of the liquid metal it also increases the time required to eventually reverse the deformation by removing the oxide. In the example shown in Figure 8 the oxidizing voltage was removed after approximately 800 ms, and although the NaOH solution immediately begins to dissolve the oxide layer this process can take anywhere from tens of seconds to several minutes before the mechanical stability is compromised. To maintain the deformation for longer periods of time, the oxidizing bias can be periodically applied in short bursts to restore the oxide that has been removed by the electrolyte.

To reverse the process, a small positive voltage is applied, which rapidly reduces the oxide layer at the leading edge and defeats the mechanical stability provided by the oxide [13]. This voltage also restores ECA conditions in the channel, which re-initiates flow for the bulk liquid metal even before the oxide layer has been fully reduced. For this reason the positive bias must be applied in short (tens of milliseconds) bursts to prevent the liquid metal from exiting the channel or stretching to the point of breaking before the oxide has been completely removed. The length of time required for this process varies depending on the thickness of the oxide layer and the extent of liquid metal intrusion into the channel, but in our tests was generally on the order of 4 to 5 seconds (recapillarity for the example shown in Figure 8 took approximately 2 seconds).

## Conclusion

Electrocapillary actuation is demonstrated to be an effective means of inducing motion in a liquid-metal droplet trapped in a quasi-planar ($w >> h$) configuration. The channel geometry maximizes the ratio of surface-area-to-volume of the liquid metal, increasing its sensitivity to surface-tension manipulation. The shape of the liquid metal can be distorted with low-voltage, low-power (~1 to 2 mW) signals that generate pressure by creating surface-tension minima on the face of the liquid metal. Once the liquid metal is distorted, voltage-controlled oxide formation can be used as a switch to maintain the shape of the liquid metal. This process can be quickly and completely reversed by reducing the oxide with a small DC bias of opposite polarity [13].

We believe this method can be used as a low-power means of controlling the shape of a liquid-metal droplet, and has applications for microfluidics, DC and RF switching, optics, and tunable RF devices, such as an RF filter with a tunable passband [11].

#### Competing interests

The authors declare that they have no competing interests.

#### Authors' contributions

RG developed the actuation technique, planned and carried out testing, and drafted the manuscript. AM and JD participated in design development, performed device fabrication and testing, and reviewed the test results. MM fabricated test fixtures and performed velocity testing of the actuation method. WS and AO guided design development and reviewed all test methods and results. All authors participated in editing the manuscript, and have read and approved the final version.

#### Acknowledgements

This work was supported by the National Science Foundation under Grant ECCS-1101936.

Received: 31 December 2014 Accepted: 11 March 2015
Published online: 28 April 2015

#### References

1. Rodrigo D, Jofre L, Cetiner B (2012) Circular beam-steering reconfigurable antenna with liquid metal parasitics. IEEE Trans Antennas Propag 60:1796–1802
2. Mumcu G, Dey A, Palomo T (2013) Frequency-agile bandpass filters using liquid metal tunable broadside coupled split ring resonators. IEEE Microw Wirel Components Lett 23:187–189
3. Jackel J, Hackwood S, Veselka J, Beni G (1983) Electrowetting switch for multimode optical fibers. Appl Opt 22:1765–1770
4. Chossat J-B, Park Y-L, Wood R, Duchaine V (2013) A soft strain sensor based on ionic and metal liquids. IEEE Sens J 13:3405–3414
5. Sen P, Kim C-J (2009) A liquid–solid direct contact low-loss RF micro switch. J Microelectromechanical Syst 18:990–997
6. Beni G (1982) Continuous electrowetting effect. Appl Phys Lett 40:912–914
7. Tsai J, Ho C-M, Wang F-C, Liang C-T (2009) Ultrahigh contrast light valve driven by electrocapillarity of liquid gallium. Appl Phys Lett 95:251110
8. Khan M, Eaker C, Bowden E, Dickey M (2014) Giant and switchable surface activity of liquid metal via surface oxidation. Proc Natl Acad Sci U S A 111:14047–14051
9. Liu T, Sen P, Kim C-J (2012) Characterization of nontoxic liquid-metal alloy Galinstan for applications in microdevices. J Microelectromechanical Syst 21:443–450
10. Keizer J, Rock P, Lin S-W (1979) Analysis of the oscillations in "beating mercury heart" systems. J. Am. Chem. Soc. 101:5637–5649
11. Gough R, Dang J, Morishita A, Ohta A, Shiroma W (2014) Reconfigurable coupled-line bandpass filter with electrically actuated liquid-metal tuning.

In: Proceedings of the 2014 Asia Pacific Microwave Conference, IEEE, Sendai, Japan, 932-934. 4–7 November 2014.
12. Ladd C, So J-H, Muth J, Dickey M (2013) 3D printing of free standing liquid metal microstructures. Adv Mater 25:5081–5085
13. Khan M, Trlica C, Dickey M (2014) Recapillarity: electrochemically controlled capillary withdrawal of a liquid metal alloy from microchannels. Adv. Funct. Mater. doi: 10.1002/adfm.201403042
14. Lee J, Kim C-J (2000) Surface-tension-driven microactuation based on continuous electrowetting. J Microelectromechanical Syst 9:171–180
15. Beni G, Hackwood S (1981) Electro-wetting displays. Appl Phys Lett 38:207–209
16. Lautrup B (2011) Surface Tension. In: Physics of Continuous Matter, 2nd edn. CRC Press, Boca Raton
17. Gough R, Morishita A, Dang J, Hu W, Shiroma W, Ohta A (2014) Continuous electrowetting of non-toxic liquid metal for RF applications. IEEE Access 2:874–882
18. Turrell F (1946) Appendix A. In: Tables of surfaces and volumes of spheres and of prolate and oblate spheroids, and spheroidal coefficients, 1st edn. University of California, Berkeley